HAL
open science

Tunnel transport through CoFe2O4 barriers investigated by conducting atomic force microscopy

M Foerster, F Rigato, K Bouzehouane, J Fontcuberta

To cite this version:

M Foerster, F Rigato, K Bouzehouane, J Fontcuberta. Tunnel transport through CoFe2O4 barriers investigated by conducting atomic force microscopy. Journal of Physics D: Applied Physics, 2010, 43 (29), pp.295001. 10.1088/0022-3727/43/29/295001 . hal-00569654

HAL Id: hal-00569654

https://hal.science/hal-00569654v1

Submitted on 25 Feb 2011

HAL is a multi-disciplinary open access archive for the deposit and dissemination of scientific research documents, whether they are published or not. The documents may come from teaching and research institutions in France or abroad, or from public or private research centers.

L'archive ouverte pluridisciplinaire **HAL**, est destinée au dépôt et à la diffusion de documents scientifiques de niveau recherche, publiés ou non, émanant des établissements d'enseignement et de recherche français ou étrangers, des laboratoires publics ou privés.

Tunnel transport through $CoFe_2O_4$ barriers investigated by conducting atomic force microscopy

M Foerster[1], F Rigato[1], K Bouzehouane[2] and J Fontcuberta[1]

[1] Institut de Ciència de Materials de Barcelona (ICMAB-CSIC), Campus UAB, 08193 Bellaterra, Spain

[2] Unité Mixte de Physique CNRS/Thales, Route Départementale 128, 91767 Orsay, France

E-mail: mfoerster@icmab.es

Abstract. Conducting atomic force microscopy has been used to monitor the quality of spin-filtering $CoFe_2O_4$ tunnel barriers by mapping current as a function of their thickness. We show that appropriate film annealing leads to a substantial improvement of their tunnelling properties. The contact force between tip and sample was identified to have a determining influence on the width of the distribution P(*I*) in current maps, thus precluding its reliable use to infer barrier characteristics. Therefore, assessment of tunnel transport should be done by means of the typical current which is a well defined parameter at a given contact force, rather than by the current distribution width.

PACS: 75.47Lx; 73.40.Gk; 81.40.Rs; 68.37Ps

1.Introduction

Spin filters, formed by a ferromagnetic insulating layer sandwiched between two normal metal electrodes, are expected to constitute spin polarized sources of relevance in future spintronics devices [1]. Spinel ferrites such as $NiFe_2O_4$ and $CoFe_2O_4$ are being considered for this purpose and recently, spin filtering effects have been demonstrated using these materials [2-5]. However, as the reported spin filtering efficiency is much below expectations, questions concerning the quality/homogeneity of the spinel barriers and on their effective height arise.

Characterization of tunnel devices is far from simple, as local variations of the tunnel barrier properties may produce large variations in conductance due to its extremely non-linear dependence on the barrier characteristics. Therefore the knowledge of barrier properties at submicronscale is of the highest relevance. Atomic force microscopy with a conducting tip (C-AFM) is a suitable tool to analyze electric transport across nanometric barriers. Current mapping at a given bias voltage (V) has been used to determine the dependence of the conductance of different barriers as a function of their thickness (t), eventually confirming tunnel transport across them [2,3]. Also attempts have been made to infer barrier characteristics from current maps recorded at different voltages, e.g. the altitude of the effective tunnel barrier [6] or the nanoscopic roughness of the barriers [7]. Typically, current maps contain a distribution of current values P(I) whose width reflects the homogeneity of the barrier properties [7-10]. For instance, it has been predicted that a Gaussian distribution of thicknesses of width σ should produce a log-normal P(I) distribution whose width is directly related to the ratio σ/λ, where λ is the electronic attenuation length in the barrier [8]. This relation is remarkable as it reveals that a tunnel barrier extremely homogeneous in thickness (σ/t <<1) may still be rough in terms of electron tunnelling if σ/λ >>1. Therefore, the analysis of the P(I) distribution may provide a deeper insight into the properties of tunnel barriers. We strengthen that reliable analysis of $I(V)$ characteristics, as measured by C-AFM, requires the use of a good metallic contact between the tip and the probed material, which cannot be commonly achieved unless the film surface is metal-capped [11].

In this work we present a detailed analysis of current maps of $CoFe_2O_4$ (CFO) barriers as a function of thickness, growth and measuring conditions, namely the applied voltage and the contact

force F_m between the tip and the sample. We show that a suitable annealing process allows improvement of their tunnel properties. Using such improved CFO barriers, we critically revise the analysis of the P*(I)* distribution as a tool to determine barrier properties and demonstrate the crucial influence of the tip-sample contact force F_m not only on the absolute current scale of P*(I)* but also on its width. Therefore, when comparing films of different thicknesses, assessment of tunnel transport should be done by means of the typical current which is a well defined parameter at a given contact force, rather than by the current distribution width.

2. Experimental details

$CoFe_2O_4$ thin films of thicknesses ranging from t = 2 nm to 8 nm were grown on a $SrRuO_3$-bottom electrode (25 nm) on $SrTiO_3$(111) single crystalline substrates by rf-sputtering. Growth conditions and structural and magnetic characterization of the films will be reported elsewhere [12]. Two series of films, denoted "*as-prepared*" and "*annealed*" where grown under the same nominal conditions. While *as-prepared* films were cooled down to room-temperature after growth, *annealed* films were kept at growth temperature (450 ºC) in 350 mTorr oxygen for 2 h before cooling down. The C-AFM measurements have been performed using a Nanotec Cervantes microscope and Nanosensors CDT-NCHR conducting tips. All scans were done with the same lateral tip speed of about 3 μm/s under N_2 atmosphere. The $SrRuO_3$ electrode was positively biased (V) and the tip was grounded. The cantilever force constant was determined from the frequency response of the free oscillation [13]. For each scan we calibrated the cantilever deflection by a deflection-displacement F(z) curve and adjusted the contact force F_m. The simultaneously recorded topographic images (see inset of figure 1d for a typical image) indicate a rms roughness below 0.2 nm for all films, slightly smaller than that measured in dynamic mode ($\sigma \sim 0.3$ nm), reflecting their extreme flatness (the unit cell of $CoFe_2O_4$ is ~0.8 nm).

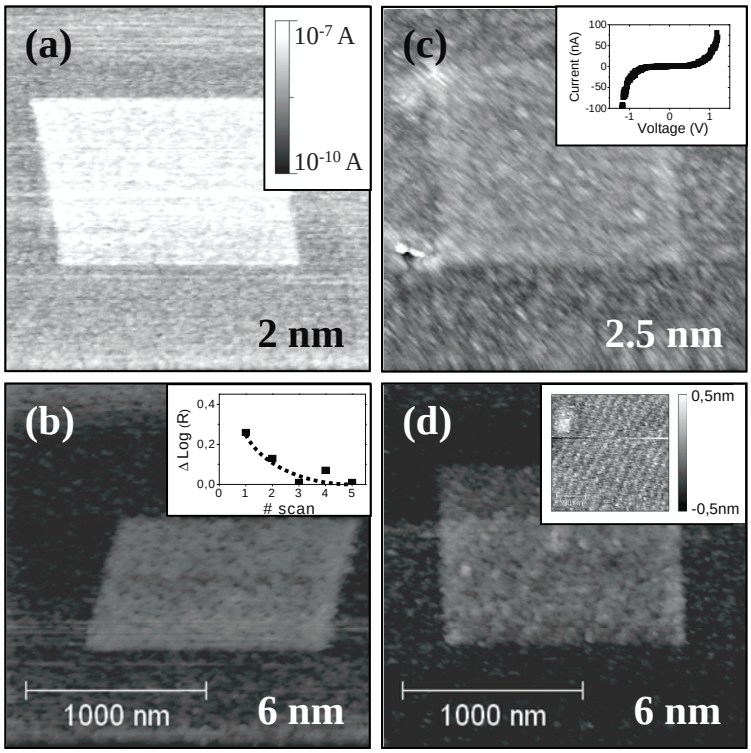

Figure 1: Current maps of films of *as-prepared* (left) and *annealed* (right) samples of various thicknesses measured at V = 0.6 V and 1 V respectively. The different contrast observed in each figure corresponds to the changes in current flow after consecutive current mapping scans as explained in the text. Insets: (b**)** difference of the current distribution maximum between central square and outer area vs. scan sequence; (c) illustrative *I-V* characteristic indicating tunnel transport; (d) typical topographic image displaying substrate induced steps.

3. Results and discussion

In figure 1 we show typical current maps obtained for *annealed* samples (right panels, measured at 1 V and 300 nN) and for the as-prepared samples (left panels, 0.6 V and 600 nN respectively). The colour contrast denotes the changes of conductance. Using a new batch of tips for the characterization of the *annealed* series, the contact force F_m had to be reduced to 300 nN since samples showed signs of indentation after applying 600 nN. In all images two well defined regions can be distinguished: The central *square* corresponds to the area that had been scanned by the tip in a preliminary scan, while the complete image is the current map measured during a subsequent larger-area scan. We ascribe the difference in conduction between the two areas to a cleaning of the sample surface by the tip during the first scan. Note that in the measurements used for current maps, there are no marks in the corresponding topography image. Further, this difference is independent of the voltage applied during the first scan (also for 0 V) and disappears after 2-3 subsequent scans (see inset in figure 1b), ruling out indentation or electronic modification of the surface as possible origin for such difference. All data

presented in this work were obtained from only the cleaned, central area. *I-V* curves recorded in a fixed point (see inset in figure 1c) show the characteristic shape of tunnel transport.

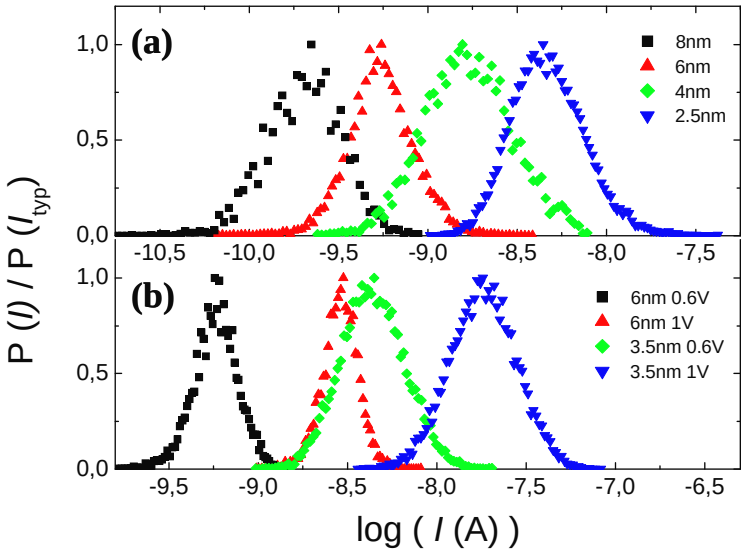

Figure 2: Normalized probability distribution P(*I*) *vs* log (*I*) of local currents in: (a) *annealed* films of different thicknesses (F_m = 300 nN, *V* = 1 V) and (b) *as-prepared* films (F_m = 600 nN) of various thicknesses and different measuring bias voltage.

Figure 2a shows the probability distribution P(*I*) of local current values for films of the *annealed* series (*V* =1 V). The shift of I_{typ} (I_{typ} is the current at which P(*I*) is maximum) towards higher values when reducing *t* corresponds to the exponential dependence of *I* on *t* which is a signature of tunnel transport and can be more clearly seen in figure 5 below. In figure 2b we show data corresponding to *as-prepared* samples measured at various bias voltages, using F_m = 600 nN. In addition to the thickness dependence, when increasing the measuring voltage there is the expected shift to higher currents of P(*I*), but without influencing its shape. As can be better appreciated in the scaling of figure 3, for all samples P(*I*) displays a tail towards high current values.

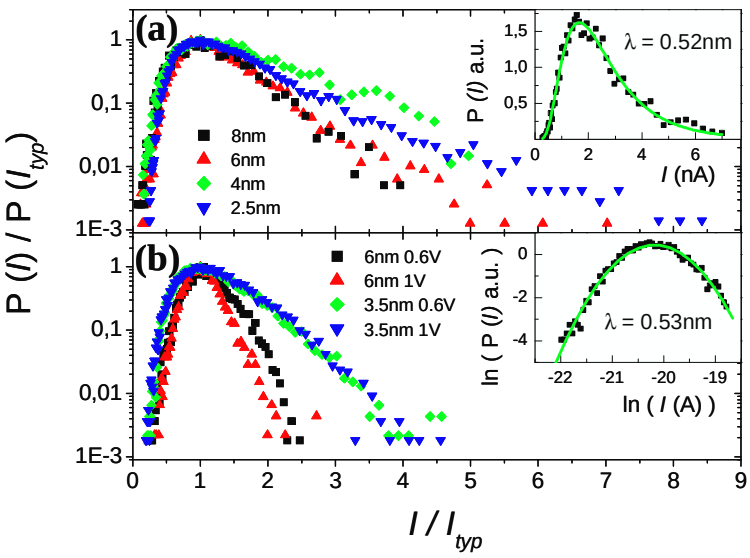

Figure 3: Logarithmic probability distributions P(*I*) of films (*annealed*, upper panel and *as-prepared*, lower panel) of Figure 2 emphasizing high current tails. Insets in (a) and (b) are examples of different fits to the same illustrative data (*annealed*, 4 nm) as described in the text.

Turning to a more quantitative description, we consider a Gaussian distribution (σ) of local barrier thicknesses. Then P(*I*) should be a log-normal distribution [8]:

$$P(I) = \frac{1}{I\beta\sqrt{2\pi}} \exp\left[-\frac{(\ln I - \mu)^2}{2\beta^2} \right] \qquad (1)$$

where μ is a scale parameter; the shape parameter (width) β is given by $\beta = \sigma/\lambda$ where λ is the barrier electronic attenuation length and σ is taken as the roughness of the film. Notice that a narrow P(*I*) distribution implies a smaller β and thus, for a given roughness, a larger λ. Based on the relation $\beta = \sigma/\lambda$, and using values of λ estimated from the expected potential barrier height (either from literature or IV curve fitting), remarkable low barrier thickness variations, typically below 0.1 nm and much smaller than the respective surface roughness have been reported for different materials [7].

To extract β and thus λ from our data presented in figure 2, the P(*I*) distribution was fitted using equation (1) (inset figure 3a). According to Refs. [8], the P(*I*) distribution can be better fitted using the log-log data representation (inset figure 3b). Both methods lead to excellent fits and similar λ values. All λ values extracted from the log P(*I*)-log (*I*) data of *annealed* and as-prepared films at different voltages are collected in figure 4a.

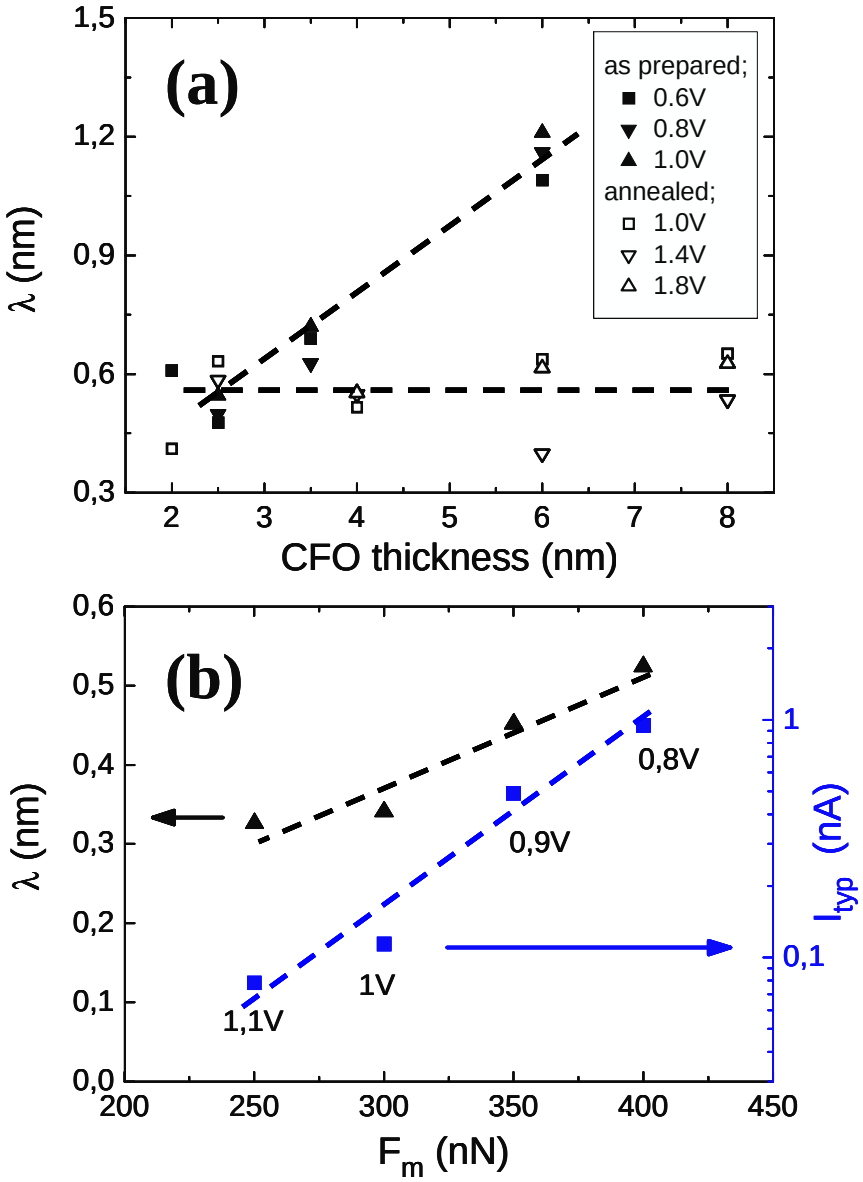

Figure 4: (a) Attenuation length λ values extracted from the log P(*I*)-log (*I*) data of all films of the *annealed* series (measured at F_m = 300nN) and *as-prepared* series (measured at F_m = 600nN). Data extracted from the P(*I*) distributions measured at different bias voltages are included. (b) Attenuation length λ(nm) of the t = 4 nm film (*annealed* series) extracted from current distributions P(I) measured at various forces F_m (triangles). The force dependence of I_{typ} for the same film is also shown (squares). In (a) and (b), dashed lines are guides to the eye.

Inspection of data in figure 4a reveals some important insights. Firstly, for both series of samples the λ values vary only slightly with *V*. As in the most simple description [8], $\lambda \sim (V_0\text{-}V)^{-(1/2)}$, the observed weak dependence of λ on *V* could be an indication that the used bias voltage *V* (~1V) is much smaller than the barrier height V_0, which however is in disagreement with the predicted band

gap of CFO (≈ 0.8V) [14]. Secondly, for *annealed* films λ is roughly constant (~ 0.6 nm) which indicates that all films have very similar barrier height and roughness. One notices that $\lambda \sim \sigma$, implying that although the films are extremely smooth ($t/\sigma > 6$), from the point of view of their electronic transparency they are not so and thus roughness still may play an important role on the tunnel transport. Finally, we notice that for the *as-prepared* films, λ increases gradually as a function of thickness thus suggesting a change in the electronic properties of these barriers with thickness.

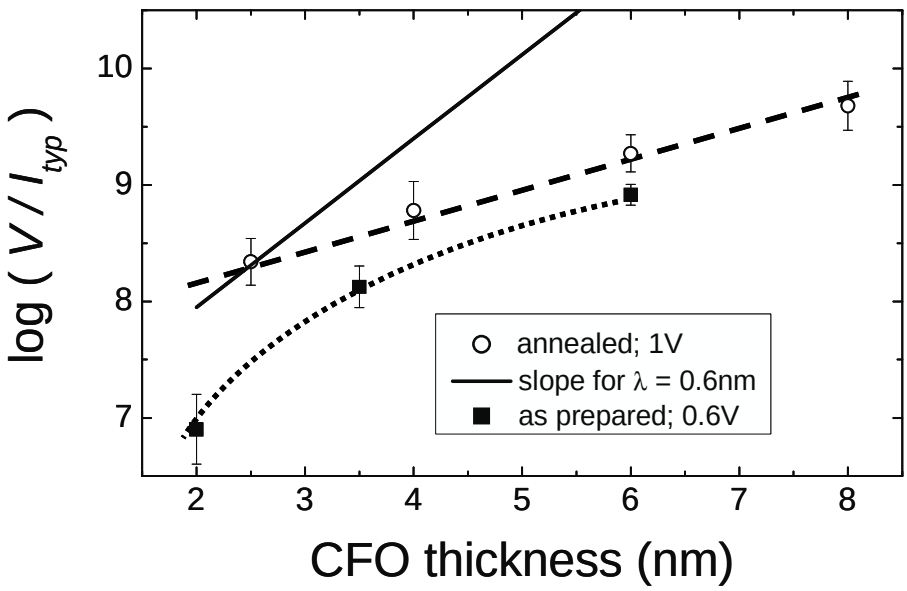

Figure 5: Thickness dependence of I_{typ} of films of the *annealed* and *as-prepared* series, as determined from P (*I*) at 1 V and 0.6 V respectively. IThe expected dependence for *annealed* samples with λ = 0.6 nm is also shown (continuous line). Dashed and dotted lines are guides to the eye.

It is a common practice to use the thickness dependence of I_{typ}, which is expected to be exponential ($I_{typ} \sim \exp[-t/\lambda]$), to assert the tunnel character of transport across thin barriers. In figure 5 we show the data corresponding to our films, determined from distributions such as those of figure 2. It is clear that *annealed* films display an exponential decrease of conductance with thickness in agreement with the constancy of the attenuation length shown in figure 4a. The decrease of conductance of *as-prepared* films with increasing *t* is sub-exponential, which is in agreement with the increase of λ with

thickness. We conclude that the process used to obtain *annealed* samples has improved the electronic properties by homogenizing the tunnel barrier.

Thus we may use the data obtained on the annealed samples (constant λ(t), exponential I_{typ}(t)) to check the validity of the relation $\beta = \sigma/\lambda$, which reveals important inconsistencies. First, as mentioned before, a stronger systematic dependence of λ on the applied voltage is expected in terms of electron tunnelling, since the applied voltage will lower the average barrier height. Second, the attenuation length λ extracted from the current map distributions is inconsistent with the experimental thickness dependence $I_{typ} \sim \exp(-t/\Lambda)$ shown in figure 5 (dashed line), which is characterized by Λ. The solid line in figure 5 indicates the $\log(V/I_{typ})$ *vs. t* slope expected from the measured attenuation length values ($\lambda \sim 0.6$ nm). From the comparison of the experimental and the predicted slope it is clear that the λ value extracted from the current maps does not reproduce the observed thickness dependence of the tunnel barrier conductance. In fact, a much larger value of $\Lambda \sim 1.8$ nm is needed to describe the experimental thickness dependence of I_{typ}. This observation implies that the experimentally measured width of P(I) is larger than expected from electronic roughening ($\sim \sigma/\lambda$) and rather determined by other, probably experimental, conditions. We will identify in the following, the contact force F_m as a main influence on the distribution width.

The applied contact force is a most critical parameter in C-AFM, since it ultimately determines the contact area and stability and therefore strongly influences experimental noise. We measured the current distribution P(I) of *annealed* samples at various F_m, and indeed observed a shrinking of the width of P(I) when increasing F_m. Consequently, the extracted attenuation length λ increases as shown in figure 4b. It has to be concluded that despite of excellent fits of all measured P(I) to log-normal distributions the current distribution width cannot be used to extract the electronic attenuation length.

4. Summary

In conclusion, we have used C-AFM to monitor the quality of the $CoFe_2O_4$ tunnel barriers, demonstrating a substantial improvement of their tunnelling characteristics through an appropriate annealing process. This is of highest significance for further spin-filter development. For improved

$CoFe_2O_4$ barriers, the analysis of distributions P(*I*) measured in current maps for different voltages and barrier thicknesses, by applying the commonly used model of statistical thickness variations, revealed inconsistencies. The contact force was identified as having a crucial influence on the current distribution width; it thus follows that the attenuation length λ extracted by using such model is not a characteristic parameter of the barrier but is strongly dependent on the measuring conditions. Therefore, assessment of tunnel transport should be done by means of the typical current which is a well defined parameter at a given contact force, rather than by the current distribution width.

Financial support by the Spanish Government (Projects MAT2008-06761-C03 and Nanoselect CSD2007-00041) and the European Union (Projects MaCoMuFi (FP6-03321) and FEDER) is acknowledged.

References

[1] Moodera J S, Hao X, Gibson G A and Meservey R 1988, *Phys. Rev. Lett.* **61** 637

[2] Lüders U, Bibes M, Bouzehouane K, Jacquet K, Contour J P, Fusil S, Bobo J F, Fontcuberta J, Barthélémy A and Fert A 2006 *Appl. Phys. Lett*, **88** 082505

Lüders U, Barthélemy A, Bibes M, Bouzehouane K, Fusil S, Jacquet E, Contour J P, Bobo J F, Fontcuberta J and Fert A 2006 *Adv. Mater.* **18** 1733

[3] Gajeck M, Bibes M, Barthélémy A, Bouzehouane K, Fusil S, Varela M, Fontcuberta J and Fert A 2005 *Phys. Rev.* B **72** 020406(R)

[4] Ramos A. V, Guittet M J, Moussy J B, Mattana R, Deranlot C, Petroff F and Gatel C 2007 *Appl. Phys. Lett.* **91** 122107

Ramos A V, Santos T S, Miao G X, Guittet M J, Moussy J B and Moodera J S 2008 *Phys. Rev.* B **78** 180402(R)

[5] Chapline M G and Wang S X 2006 *Phys. Rev.* B **74** 014418

[6] Infante I C, Sánchez F, Laukhin V, Pérez del Pino A, Fontcuberta J, Bouzehouane K, Fusil S and Barthélémy A 2006 *Appl. Phys. Lett.* **89** 172506

[7] Da Costa V, Bardou F, Béal C, Henry Y, Bucher J P and Ounadjela K 1998 *J. Appl. Phys.* **83** 6703

Da Costa V, Henry Y, Bardou F, Romeo M and Ounadjela K 2000 *Eur. Phys. J.* B **13** 297

Da Costa V, Tiusan C, Dimopoulos D and ounadjela K 2000 *Phys. Rev. Lett.* **85** 876

Gilles B, Fettar F, Pillet J C, Marty A, Ernult F, Monso S and Dieny B 2002 *J. Mag. Mag. Mat.* **242** 1261

Fix T, Da Costa V, Ulhaq-Bouillet C, Colis S, Dinia A, Bouzehouane K and Barthélemy A 2007 *Appl. Phys. Lett.* **91**, 083104

[8] Da Costa V, Romeo M and Bardou F 2003 *J. Mag. Mag. Mater.* **258** 90

Bardou F 1997 *Europhys. Lett.* **39** 239

[9] Ando Y, Kameda H, Kubota H and Miyazaki T 2000 *J. Appl. Phys.* **87** 5206

Dimopoulos T, Da Costa V, Tiusan C, Ounadjela K, van der Berg H A M 2001 *J. Appl. Phys.* **89** 7371

[10] Lang K M, Hite D H, Simmonds R W, McDermott R, Pappas D P and Martinis J M 2004 *Rev. Sci. Instrum.* **75** 2726

[11] Worledge D C and Abraham D W 2003 *Appl. Phys. Lett.* **82** 4522

[12] Rigato F, Foerster M and Fontcuberta J, submitted for publication.

[13] Sader J E, Chon J W M and Mulvaney P 1999 *Rev. Sci. Instrum.* **70**, 3967

[14] Szotek Z, Temmerman W M, Ködderitzsch D, Svane A, Petit L and Winter H 2006 *Phys. Rev.* B **74** 174431